Sensors & Transducers

Synergistic Effect of L-Methionine and KI on Copper Corrosion Inhibition in HNO$_3$ (1M)

Amel SEDIK, Sihem ABDERRAHMANE, Said BOUKERCHE, Abdelaziz HIMOUR and Amel GHARBI

Laboratoire d'Ingénierie des Surfaces (LIS) -Université Badji Mokhtar,
BP. 12 - 23000 Annaba, Algérie
E-mail: abderrahmanesihem@yahoo.fr

Abstract: L-Methionine (L-Met) efficiency as a non-toxic corrosion inhibitor for copper in 1M HNO$_3$ has been studied by using electrochemical impedance spectroscopy (EIS) and potentiodynamic polarization. Copper corrosion rate significant decrease was observed in the presence of L-Met at 10^{-4}M. The Obtained Results from potentiodynamic polarization and impedance measurements are in good agreement. L-Methionine adsorption on copper surface follows Langmuir isotherm. L-Met free energy adsorption on copper (-30 KJ mol^{-1}) reveals an inhibition strong physical adsorption on copper surface. In order to evaluate the L-Met effect, L-Met and iodide ion'synergistic effect was used to prevent copper corrosion in nitric acid. It was found that inhibitor efficiency (IE) reached 98.27 % in 1M solution containing 10^{-4}M L-Met and 10^{-3} M KI. The synergistic effect was attributed to iodide ions adsorption on copper surface, which facilitated the L-Met adsorption and an inhibitive film formation. *Copyright © 2014 IFSA Publishing, S. L.*

Keywords: Corrosion, Copper, L-methionine, KI, Synergistic effects.

1. Introduction

Copper and its alloys are widely used materials for their excellent electrical and thermal conductivities in many applications, such as electronics and integrated circuits manufacture. Copper is a relatively noble metal [1], requiring strong oxidants for its corrosion or dissolution. The mostly used corrosive solution contains nitric acid; for that, this medium has induced several copper corrosion researches [2].

Different corrosion inhibitors are used to control and reduce metals' corrosion in corrosive media. Due to most inorganic corrosion inhibitors' toxicity, such as chromates and nitrites, and also because of restrictive environmental regulations; these inhibitors

are being replaced by new environmentally organic compounds. Copper corrosion in different solutions has also been effectively controlled using organic inhibitors containing nitrogen, oxygen or sulphur [3].

Amino acids form organic compounds' class whichare completely soluble in aqueous media and they are produced with high purity at reduced costs. These properties would justify their use as corrosion inhibitors.

L-Methionine was an amino acid containing both the (–NH$_2$) and (–S–CH$_3$) groups in its molecule, which has been used in different metals' corrosion inhibition. Oguzie et al [4], studied L-Methionine corrosion inhibition and adsorption behavior on mild steel in H$_2$SO$_4$ solution. The hydrodynamic conditions' Influence on L-Methionine

behavior, as a green organic inhibitor, was studied by Ashassi-Sorkhabi et al using rotating disc electrode [5]. It was shown that all corrosion parameters depended on the electrode rotation rate. Synergistic inhibition effect (synergism) is a combined compounds' action greater in total effect than the individual effects' sum. Corrosion inhibitors' synergism is either due to interaction between inhibitor composition components or due to interaction between the inhibitor and one of the ions present in aqueous solution [6]. Synergism is an effective method used to: improve the inhibitor efficiency, decrease the usage amount and diversify the inhibitor application in acidic media. It has a primordial role not only in corrosion inhibitors'theoretical research but also in practical work [7].

It is generally observed that [8] the halide ions' addition to the corrosive media increases the organic cations adsorption ability by forming interconnecting bridges between negatively charged metal surface and inhibitor cations. And synergistically, it also increases significantly organic compounds inhibition efficiency. The halide ions' synergism order is I⁻ > Br⁻ > Cl⁻. Since it has larger size and easy polarizability, I⁻ ions are chemisorbed on metal surface and provide better synergistic effect [9]. Synergism is indeed an effective approach to enhance the inhibitors' effect to decrease the organic compounds' dosage and to diversify the inhibitors' application in acid media.

In the literature, there are several reports dealing with synergistic inhibition mechanism. Zhang and al. [10] explained the synergistic inhibition effect by iodide ions' initial contact adsorption on copper surface, followed by a positive charge decrease on metal, which enhances 2-mercapto benzimidazole adsorption on copper.

Wu et al, [11] proposed that copper improved corrosion inhibition in 0.5 M H_2SO_4+0.01M benztriazole (BTAH) + 0.01 M KI solution due to $BTAH_2^+$ adsorption on copper surface and new Cu(IBTA) complex film formation through a covalent bond between BTAH and iodide ions. Zhang et al, [12] explained the higher inhibition efficiency of Arginine self-assembled monolayer in KI presence by I⁻ ions' adsorption on copper surface and the interconnecting bridges forming between copper surface and the positive centre in arginine molecules, which facilitates the adsorption.

Another explanation of iodide ions improved inhibition efficiency is the iodide ions presence causing a positive shift in zero charge potential and makes more negative overall charge on metal surface, which facilitates positively charged species adsorption [11].

In this present work, we have studied L-Methionine inhibition effect on copper corrosion in 1 M HNO_3 solution. Then, we attempted to increase the inhibition efficiency synergistically further by the iodide ions addition to the L-Methionine containing corrosive solution.

2. Experimental Procedures

2.1. Materials

Nitric acid (1 M HNO_3) solutions were prepared by analytical grade 86 % HNO_3 dilution with distilled water. The used inhibitor in this study was L-Methionine.

(CH_3–S–CH_2–CH_2–CH(COOH)NH_2), which was obtained from SIGMA (Life Science) Company. The inhibitor used concentration in aggressive solution was 10^{-2}, 10^{-3} and 10^{-4}M (Fig. 1). The halide salt, potassium iodide (KI) used was in the concentration range 10^{-1}-10^{-4} M; however, 10^{-3} M KI was used for the synergistic study. The solution volume was fixed at 150 ml.
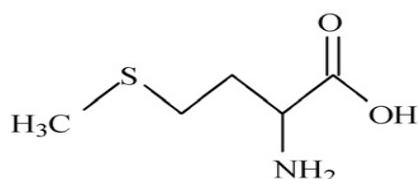
Fig. 1. L-Methionine structure.

The working electrode (WE) for the potentiodynamic curves and EIS measurements was prepared from cylindrical copper rod (99.99 %) sealed with epoxy resin (1.33 cm^2) sectional area. The specimens' surface preparation was carried out using different grades emery papers (#600, #1200and #2400), and polished with diamond paste (3 μm). Then it was degreased with acetone, rinsed with distilled water and dried under airflow.

The reference electrode was a saturated calomel electrode (SCE) and a platinum electrode was used as auxiliary electrode. All reported potential values were referred to this electrode type. Electrochemical experiments were carried out under static conditions at 25°C.

2.2. Apparatus

The experimental device used for electrochemical measurements was Gamry reference 600 associated with logiciel Gamry Framwork.

2.3. Procedures

2.3.1. Potentiodynamic Polarization Measurements

The working electrode was immersed in a test solution for 2 h until a stable open-circuit potential was attained. Potentiodynamic polarization studies were carried out in the potential range −600 mV to +800 mV with 1 mVs⁻¹ scan rate.

2.3.2. EIS Measurements

The EIS experiment was performed at open circuit potential over a 100 kHz to 10 MHz frequency range. The sinusoidal potential perturbation was 5 mV in amplitude.

Fig. 3. Potential–pH equilibrium diagram for the system, copper–water, at 25 C. The dashed regions and the equilibrium components corresponding to the Pourbaix diagram in HNO₃.

The electrochemical reactions for copper in HNO_3 solution can be described as follow.
Anodic reaction:

$$Cu \leftrightarrow Cu(I)_{ads} + 1\ \bar{e} \qquad (1)$$

$$Cu(I)_{ads} \leftrightarrow Cu(II) + 1\ \bar{e} \qquad (2)$$

$Cu(I)_{ads}$ is adsorbed on copper metal surface and does not diffuse into the solution. For that, copper dissolution is controlled by $Cu(II)_{ads}$ soluble species diffusion [16].
Cathodic reactions:

$$NO_3^- + 3H^+ + 2\bar{e} \rightarrow HNO_2 + H_2O \qquad (3)$$

$$NO_3^- + 4H^+ + 3\bar{e} \rightarrow NO + 2H_2O \qquad (4)$$

$$O_2 + 4H^+ + 4\bar{e} \rightarrow 2H_2O \qquad (5)$$
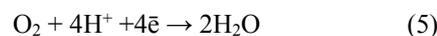
Some works on copper reduction in HNO_3 reports that in copper ions (II) presence, NO is the main product, but the NH_3 becomes dominant in their absence. It appears that in nitric acid diluted solutions, copper oxidation is an electrochemical reaction; on the other hand, it becomes a chemical reaction in concentrated medium [17]. It should be noted that the literature does not report experimental evidence on intermediary product nature. It is observed that, in all cases (Fig. 4), the E_{Corr} values show slight shifts in negative directions, while both the cathodic (b_c) and anodic (b_a) Tafel slopes increase. These effects are significantly enhanced upon decreasing the L-Met concentration.

Therefore, these latter results reveal that L-Methionine presence in HNO_3 solution inhibits both the anodic and cathodic processes (mixed-inhibitors). Based on these results, the compound action may be related to adsorption and barrier film formation on copper surface, impeding both cathodic and anodic sites [18]. For cathodic polarization curves, in the potential range between −0.25 and −0.65 V, the current plateau can be ascribed to dissolved oxygen reduction, limited by natural convection diffusion.

Fig. 2. Open circuit potentials of copper in 1 M HNO₃, without and with L-Methionine at different concentrations.

3. Results and Discussion

3.1. Open-Circuit Potential Measurements

The open-circuit potential (E_{ocp}) variation with time for all samples in 1 M HNO_3 solution without and with addition of L-Methionine at different concentrations is shown in Fig. 2.

The open circuit corrosion potential reaches its steady state at about 3600 s immersion. At 10^{-4} M of L-Methionine, the potential shifts towards slightly a more negative value at the immersion beginning. This phenomenon may be attributed to the anodic process slow down, for instance due to an adsorbed film formation on the alloy surface [13].

3.2. Potentiodynamic Polarization Measurements

According to corrosion theory [14], the cathodic curves' rightward shift reveals that corrosion is mainly accelerated by cathode reactions. HNO_3 is a strong copper oxidizer capable of copper rapid attacking. The Pourbaix diagram for copper–water system is drawn on Fig. 3 [15]. It indicates that copper is corroded to Cu^{2+} in HNO_3 solutions, and no oxide film is formed to protect the surface from corrosion.

Fig. 4. Anodic and cathodic Tafel polarization curves for copper in 1 M HNO$_3$ without and with various concentrations of L-Methionine after immersion for 2 h.

The dissolved oxygen reduction reaction can be expressed by equation (5). At potentials below −0.85 V, further cathodic current density increase is observed. This current associated process

corresponds to hydrogen evolution, and is represented by the reaction:

$$2H_3O^+ + 2e^- \leftrightarrow H_2 + 2H_2O \tag{6}$$
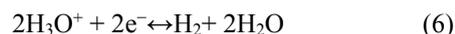
The obtained electrochemical parameters from copper polarization curves in 1 M HNO$_3$ solution with and without L-Methionine are grouped in Table 1. The polarization resistance values, derived from polarization curves, allow to calculate the inhibitive efficiency, according to the equation:

$$\eta\ (\%\ ) = [1 - (\ R_p / R_p^{'})] \times 100, \tag{7}$$

where Rp and R$'_p$ are the polarization resistance values of copper without and with L-Methionine, respectively.

We note that the inhibitor concentration decrease when inhibitive efficiency increase, that reaches a maximum value of 95.75% for L-Methionine 10^{-4} M.

Table 1. Parameters obtained from potentiodynamic curves of copper in 1 M HNO$_3$ + L.Met at various concentrations.

C (M)	E_{corr} (mV/ECS)	I_{corr} (μA.cm^{-2})	b_a (mV.dec^{-1})	b_c (mV.dec^{-1})	R_p (Ohm.cm^2)	η (%)
0	-31.28	98.96	106.1	154.8	3.61	-
10^{-2}	-73.29	10.06	90.52	173.0	10.68	66.19
10^{-3}	-94.17	12.89	110.0	400.5	13.68	73.61
10^{-4}	-86.21	9.036	152.5	622.4	85.11	95.75

3.3. Electrochemical Impedance Spectroscopy (EIS)

Fig. 5a-c represents the measured impedance spectra at E$_{corr}$ after 2 h immersion, and exemplify respectively, Nyquist, bode and phase angle plots obtained for copper in 1 M HNO$_3$ solution with and without L-Met various concentrations. In all cases (Fig 5a), the impedance spectra are characterized by the appearance of two not clearly resolved time constants related to the capacitive loops observed in the Nyquist plots. Copper surface was always covered with copper-oxide films formed in both the air and the aqueous solution. The semicircle at higher frequency was attributed to the oxide layer present on copper surface. The second semicircle was due to the charge transfer process [18]. Deviations from the ideal semicircles could be attributed to surface inhomogeneities [19].

It is also attributed to active sites' distribution, inhibitor molecules' adsorption and porous layers' formation [18]. Generally, measured impedance loops are often depressed semicircles with their center below the real-axis. This phenomenon kind is known as the dispersing effect. The capacitive loop size's increase with L-Methionine addition shows that a barrier gradually forms on copper surface. The

barrier is probably related to an inhibitor surface film formation on the electrode surface, as will be discussed [20].

(Fig. 5b) and (Fig. 5c) present the impedance diagrams for the same experimental data in Bode (logZ= f(logf) and Bode-phase format (logf=f(phase) in presence of inhibitor solutions different concentrations. From the Bode plots (Fig. 5b), all impedances increase with the inhibitor concentration. (Fig. 5c) shows phase angle shift continuous increase, the first maximum phase angle is about 18.2° at 15.85 MHz, and the second maximum phase angle is about 45.5° at 100.1 kHz , obviously correlating with adsorbed inhibitor decrease on copper surface.

The equivalent circuit (EC) given in Fig. 6 was used. Table 2 shows the corresponding fitted results where *Rs*is the solution resistance and *R*1 is the charge transfer resistance. *CPE*1 is the double layer capacitance. R_2 and *CPE*2 are associated with the adsorbed inhibitor [21]. Data were adjusted using constant phase element.

It is seen from Table 2 that charge transfer resistance increase and double-layer capacitance decrease, with inhibitor use, have been attributed to the inhibitor molecule enhanced adsorption on metal surface, which reduces the electrode active surface [22].
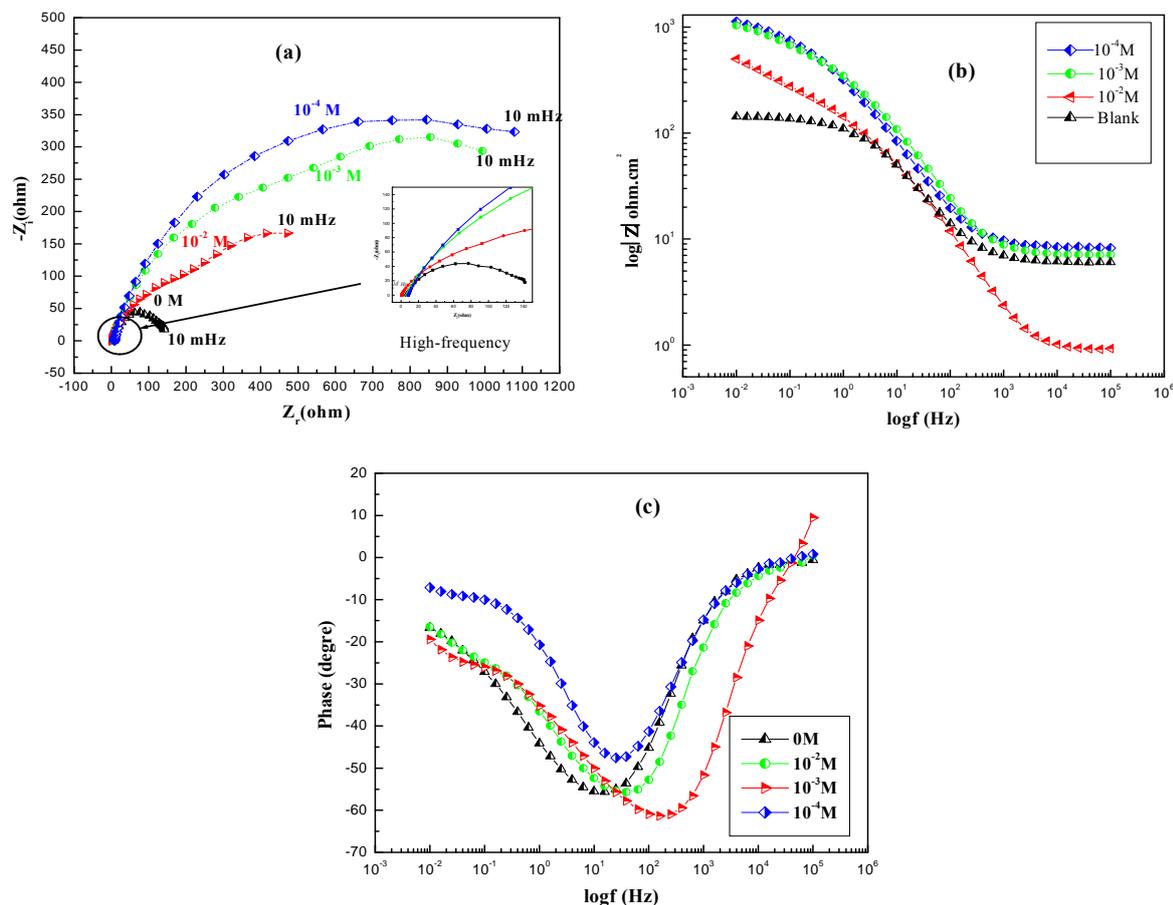
Fig. 5. Electrochemical impedance plots of copper in 1 M HNO$_3$ containing different concentrations of L-Methionine:
(a) Nyquist, (b) Bode and phaseangle plots (c).
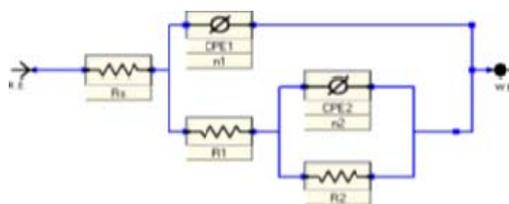
Fig. 6. Equivalent electrical circuits used to represent the impedance data of Cu in 1M HNO$_3$ solution
with and without various concentrations of L-Met.

Table 2. Parameters obtained from equivalent circuit of copper in 1 M HNO$_3$ + L.Met at various concentrations.

C (M)	Rs ($\Omega.cm^2$)	CPE1 ($\mu F.cm^2$)	n$_1$	R$_1$ ($\Omega.cm^2$)	CPE2 ($\mu F.cm^2$)	n$_2$	R$_2$ ($\Omega.cm^2$)	H (%)
0M	5.80	0.85	0.65	10.82	9.58	0.92	1.01	-
10^{-2}M	3.98	0.70	0.83	21.43	7.20	0.89	3.58	49.51
10^{-3}M	6.65	0.64	0.69	78.30	3.90	0.93	8.6	89.98
10^{-4}M	8.13	0.004	0.91	265.8	0.69	0.91	15.2	95.92

Charge transfer resistance increase resulted in metal oxidation reaction decrease at the same potential region. The *n* changes (0.65–0.91) value can be attributed, as well, to initial surface inhomogeneity decrease resulting from the inhibitor's adsorption on most active centers [19]. When the inhibitor concentration decreases, we observe that R_t increases while C_{dl} decreases. The C_{dl} decrease could be due to the inhibitor adsorption on copper metal surface, which reduces the electrode active surface. The

inhibition efficiencies, η %, were also calculated using the following relationship:

$$\eta\% = [1 - (R_t/R'_t)] \times 100, \qquad (8)$$

where R_t and R'_t are the charge transfer resistances in the absence and presence of inhibitor, respectively. This efficiency increases while the inhibitor concentration reaches 93.19 % at 10^{-4} M. maximum value.

It can be concluded that the inhibition efficiency calculated from polarization curves and electrochemical impedance spectroscopy measurements are in good agreement.

4. Adsorption Isotherm

Copper corrosion inhibition in HNO_3 acid solution by inhibitors is based on molecular adsorption. The adsorption process is influenced by organic compounds chemical structures: the charge distribution in molecule, the nature and surface metal charge and the aggressive media type [23]. Basic data on the interaction between inhibitors and copper surface can be provided by isotherms' adsorption. Totally, isotherms' adsorption provides data about the interaction among the adsorbed molecules themselves and their interactions with the electrode surface [24].

Assuming a direct relationship between inhibition efficiency (η %) and surface coverage (θ) (η % = 100 × θ) for different inhibitor concentrations, data obtained from EIS measurements were adapted to determine the adsorption characteristics of L-Methionine on copper in 1 M HNO_3 solution. To clarify the nature of adsorption, theoretical fitting to different isotherms was undertaken and the correlation coefficients (r^2) were used to determine the best fit which was obtained with the Langmuir isotherm ($r^2 = 0.995$).

The Langmuir isotherm is given by[25]:

$$\theta = \frac{KC}{KC + 1} \qquad (9)$$

where C is the inhibitor concentration, θ is the fractional surface coverage and K is the adsorption equilibrium constant related to ΔG_{ads} adsorption free energy.

The linear relationships suggest that the inhibitors' adsorption obeys to Langmuir adsorption isotherm (Fig.7). The straight line has an 1/K. Eq intercept (10) that can determine constant K relation with standard free energy:

$$K = \left(\frac{1}{55.5}\right) \exp\left(-\frac{\Delta G°ads}{RT}\right) \qquad (10)$$

The ΔG_{ads} negative values indicate that the inhibitors' adsorption on metal surface is spontaneous. Generally, ΔG_{ads} values around -20 kJ mol^{-1} or lower are consistent with the electrostatic interaction between charged both molecules and metal surface (physisorption). Those around -40 kJ mol^{-1} or higher involve charge sharing or transfer from organic molecules to metal surface in order to form metal bond coordinate type (chemisorption) [26]. This indicates that L-Methionine takes place through electrostatic interaction between the inhibitor molecule and copper surface. ΔG large negative value reveals strong physical adsorption.
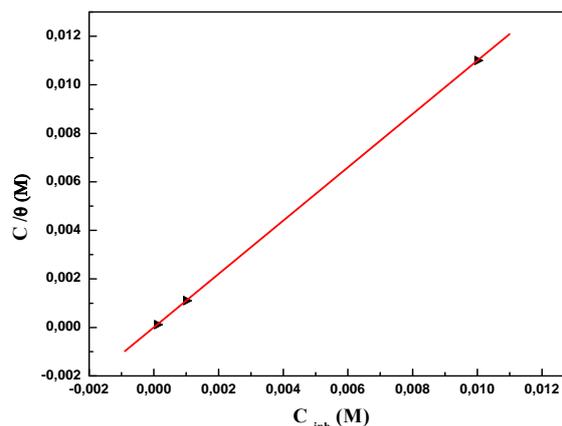
Fig. 7. Langmuir adsorption isotherm on the copper surface in nitric acid solutions containing various concentrations of L-Methionine.

5. Corrosion Inhibition of L-Methionine

In acid solution, the L-Methionine should be protonated $[CH_3-S-CH_2-CH-(NH^+_3)CO_2H]$ by net positive on both electrode surfaces and therefore, will restrict adsorption via positively charged N atom. The observed inhibiting effect can be attributed to electrons' sharing between the L-Met S atom and the electrode. When both neutral and protonated forms of the inhibitors adsorb on copper surface, coordinate bonds are formed by electrons' partial transference from the unprotonated N atoms, sulfur atoms, delocalized π electrons in inhibitor rings' molecule to metal surface via Cu^{2+} ions vacant d orbitals. So, in adsorption process, both physical and chemical adsorptions might take place [27].

K. F. Khaled [18], reported that the groups (–NH$_2$, S–CH$_3$,–S=O, –SO$_2$) can occur on positive copper surface. Protonated L-Methionine adsorption on copper surface cathodic sites will retard the oxygen evolution reaction. Copper surface adsorption on anodicsites can occur via S atom in the aliphatic chain in L-Met case, in order to retard copper dissolution process. L-Met copper surface adsorption is assisted by hydrogen bond formation between L-Methionine and the Cu_2O and/or CuO formed on copper surface. This adsorption type should be more prevalent for protonated inhibitors, because the positive charge on N-atom is conductive to hydrogen

bonds' formation. Unprotonated N-atoms may adsorb by either direct chemisorption, or by hydrogen bonding [28]. Thus, L-Methionine has the ability to influence both the cathodic and anodic partial reactions, giving rise to mixed-inhibition observed mechanism.

6. Effect of Iodide Ions

6.1. Polarization Measurements

Copper potentiodynamic polarization behaviour in 1 M HNO_3 and L-Methionine 10^{-4} M without and with KI at 10^{-3} M is shown in Fig. 8.

It is clear in this figure that iodide ions potential addition reduced both anodic copper dissolution and cathodic oxygen evolution reactions. This means that KI and L-Methionine mixture behaves as a mixed-type inhibitor for copper corrosion in nitric acid solution. Corrosion current densities (i_{corr}) were reduced in iodide ions' presence compared to its absence and were also found to be concentration dependent. The obtained corrosion kinetic parameters from these curves are given in Table 3.

Fig. 8 shows that iodide ions' addition to L-Methionine produces pronounced effects on anodic and cathodic currents compared to those obtained in only L-Methionine and E_{corr} presence do not change prominently. This indicates that copper corrosion reaction mechanism does not change. From Table 3,

it is seen that corrosion current density is reduced from 98.96 $\mu A/cm^2$ in acid solution to 9.03 $\mu A/cm^2$ in L-Met presence. These values were further reduced to 2.95 $\mu A/cm^2$ on KI introduction at 10^{-3} M. Also the inhibition efficiency was upgraded from 95.75 % obtained for L-Methionine alone to 98.27 % in KI addition to this latter. These results confirm strong synergism existence between L-Methionine and KI in copper corrosion inhibition in these solutions.
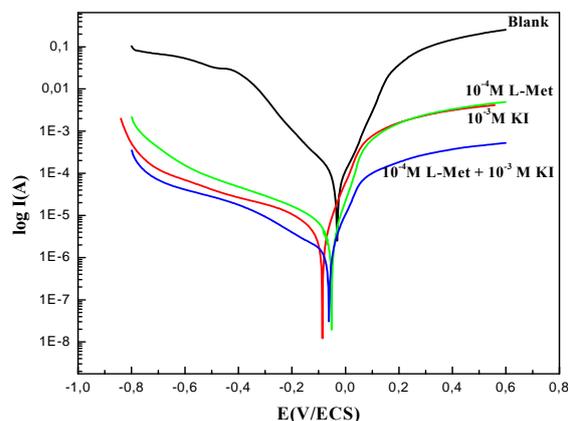
Fig. 8. Copper electrochemical polarization curves in different solutions.

Table 3. Parameters obtained from polarisation curves of copper in different solutions.

Solutions	E_{corr} (mV/ECS)	I_{corr} ($\mu A.cm^{-2}$)	b_a ($mV.dec^{-1}$)	b_c ($mV.dec^{-1}$)	R_p ($ohm.cm^2$)	η (%)
1M HNO_3	-31.28	98.96	106.1	154.8	3.61	-
1M HNO_3 + 10^{-4}M L-Met	-86.21	9.036	152.5	622.4	85.11	95.75
1M HNO_3 + 10^{-3}M KI	61.40	8.49	112.1	469.5	100.3	96.40
1M HNO_3 + 10^{-4}M L-Met +10^{-3}MKI	--51.67	2.95	176.3	622.4	208.4	98.27

6.2. Electrochemical Impedance Spectroscopy Measurements

In order to assess iodide ions addition effect on L-Met corrosion inhibition for pure copper in 1 M HNO_3; electrochemical impedance spectroscopy measurements were undertaken using L-Met (10^{-4} M) fixed concentration combined with KI (10^{-3} M). The impedance response from these systems is depicted in Fig. 9, representing the Nyquist plots. The results clearly show iodide ions addition distinct effect on copper corrosion behavior compared to the blank acid solution in L-Met absence and presence. In comparison with the L-Met alone, the semicircle size in Nyquist plot increases on iodide ions addition to L-Methionine at 10^{-3} M, and the Warburg diffusion was observed at low frequency values. Therefore, diffusion controlled process exists.

Studies reported in literature [29] showed that the diffusion process is controlled by dissolved oxygen diffusion from the global solution to the electrode surface and the Warburg impedance; which is observed in the low frequencies; it is ascribed to copper surface oxygen diffusion. This diffusion tail still appears, even in presence of tested inhibitors high concentrations. This means that copper corrosion behavior in KI absence as well as in its presence is influenced by mass transport.

The employed equivalent circuit model in 10^{-4} M L-Met presence in combination with 10^{-3}M KI is presented in Fig. 10. W stands for the Warburg impedance, R is a resistor (Rs = solution resistance, and R_{ct} = charge-transfer resistance), and CPE represents the constant phase element. Here, CPE is substituted for double-layer capacitance, C_{dl} to give more accurate fit.
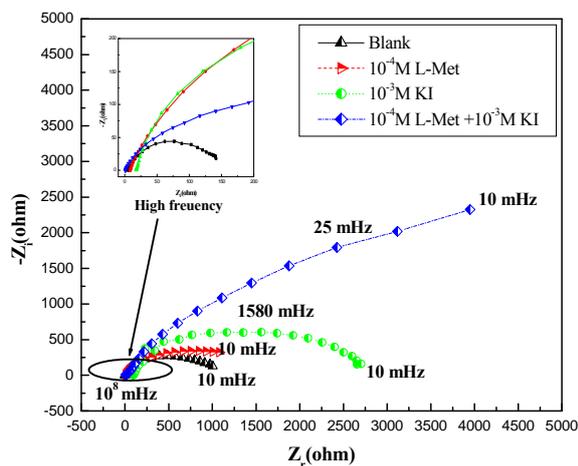
Fig. 9. Electrochemical impedance plots of copper in different solutions.

It shows that I⁻ addition increased the R_{ct} value to 265.8 Ohm to 664.5 Ohm and the inhibition efficiency has improved to 98.45% compared to L-Met alone inhibition efficiency, which is only 93.19 % (Table 4).

The calculated inhibition efficiency η (%) is also reported from Eq. (8).
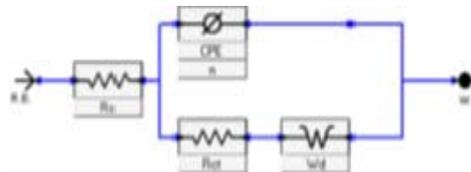
Fig. 10. Equivalent circuit model for the corrosion of copper in 1 M HNO₃ + 10⁻⁴ M L-Met + 10⁻³ M KI .

Table 4. Parameters obtained from equivalent circuit of copper in1M HNO₃+10⁻³ M KI +10⁻⁴M L.Met.

C (M)	R_s (Ωcm²)	CPE (μF.cm²)	n	W_d (μF.cm²s^{1/2})	R_{ct} (Ωcm²)	η(%)
1 HNO₃ + 10⁻⁴ L-Met +10⁻³ KI	5	0.001	0.95	750	664.5	98.45

7. Synergistic Parameter of Ions I⁻ and L-Methionine

To confirm whether synergism is taking place, a parameter (S), as initially proposed by Aramaki and Hackerman [30], for describing amines and halide ions combined inhibition behavior (Table 5). Generally, for A and B inhibitors interaction, this synergism parameter (S) is defined as follows:

$$S= (1- \eta_{A,B}) /(1- \eta'_{A,B}) \qquad (11)$$

$$\eta_{A,B}= (1-\eta_A) (1-\eta_B) , \qquad (12)$$

where η_A is the inhibition efficiency with L-Methionine; η_B is the inhibition efficiency with iodide ions and $\eta_{A,B}$ is the inhibition efficiency for the combination of L-Methionine and iodide.

When S <1: the adsorption mechanism is *competitive*, then S > 1: the adsorption mechanism is *cooperative.* This parameter was evaluated from the inhibition efficiency values obtained from potentiodynamic measurements.

Table 5. Synergism parameters (S) of copper in 1 M HNO₃ + 10⁻³M KI + L-Met at various concentrations.

C (M)	Synergistic parameter (S)	
	Polarization	Impedance
10⁻² 10⁻³ 10⁻⁴	1.02 1,03 1.15 1,65 1.57 1,61	

Table 5 data clearly demonstrate that S values are superior than unity; suggesting that synergistic action of I⁻ with CH₃-S-CH₂-CH-(NH⁺₃)CO₂H cation is due to cooperative adsorption where the anion is chemisorbed on the surface and the cation is adsorbed on the anion layer . It is obvious that S values obtained from both methods (polarization and impedance) are in good agreement.

8. Conclusion

L-Methionine influence on copper corrosion behavior in 1M nitric acid is studied and the following aspects can be emphasized:

-Potentiodynamic polarization studies have shown that L-Methionine acts as mixed-type inhibitor. For the 10⁻⁴M L-Methionine, the corrosion inhibition efficiency reaches 95.75 %.

Impedance spectra obtained in solution with and without inhibitor were characterized by two slightly distorted capacities; one at high frequency and the other at low frequency. EIS experiments also show, in 10⁻⁴ M L-Methionine solution, charge transfer resistance increase to 265.8 Ohm.cm².The corrosion inhibitive efficiency is 95.92 %.

L-Met Adsorption on copper surface obeys to Langmuir isotherm. The adsorption free energy is 30 KJ.mol⁻¹ revealing strong physical adsorption.

-Synergistic effect between L-Met and iodide ions in 1 M nitric acid has been observed. Iodide ions' addition enhances, significantly, corrosion behavior. This effect is attributed to positive surface charge, which facilitates the iodide ions' initial adsorption.

The synergistic parameters S > 1, for all cases, suggest the cooperative adsorption. The inhibitive efficiency has improved to 98 %.

Acknowledgments

References

[1]. M. A. Al-Qudah, Inhibition of Copper Corrosion by Flavonoids in Nitric Acid, *E-Journal of Chemistry*, Vol. 8, Issue 1, 2011, pp. 326-332.

[2]. A. Fiala, A. Chibani, A. Darchen, A. Boulkamh, K. Djebbar, Investigations of the inhibition of copper corrosion in nitric acid solutions by ketene dithioacetal derivatives, *Applied Surface Science*, Vol. 253, 2007, pp. 9347–9356.

[3]. D.-Q. Zhanga, Q.-R. Caib, X.-M. Heb, L.-X. Gaoa, G. S. Kimc, Corrosion inhibition and adsorption behavior of methionine on copper in HCl and synergistic effect of Zinc ions, *Materials Chemistry and Physics*, Vol. 114, 2009, pp. 612–617.

[4]. E. E. Oguzie, C. Unaegbu, C. N. Ogukwe, B. N. Okolue, A. I. Onuchukwu, Inhibition of mild steel corrosion in sulphuric acid using indigo dye and synergistic halide additives, *Materials Chemistry and Physics*, Vol. 84, 2004, pp. 363–368.

[5]. H. Ashassi-Sorkhabi, E. Asghari, Effect of hydrodynamic conditions on the inhibition performance of l-methionine as a "green" inhibitor, *Electrochimica Acta*, Vol. 54, 2008, pp. 162–167.

[6]. E. Kalman, I. Lukovits, G. Palinkas, A simple model for synergism of corrosion inhibitors, *ACH – Models Chem.*, Vol. 132, 1995, pp. 527–537.

[7]. S. S. A. Rehim, O. A. Hazzazi, M. A. Amin, K. F. Khaled, On the corrosion inhibition of low carbon steel in concentrated sulphuric acid solutions. Part I: Chemical and electrochemical (AC and DC) studies. *Corrosion Science*, Vol. 50, 2008, pp. 2258–2271.

[8]. X. Li, S. Deng, H. Fu, G. Mu, Synergistic inhibition effect of rare earth cerium(IV) ion and 3,4-dihydroxybenzaldehye on the corrosion of cold rolled steel in H_2SO_4 solution, *Corrosion Science*, Vol. 51, 2009, pp. 2639–2651.

[9]. S. A. Umorena, E. E. Ebenso, The synergistic effect ofpolyacrylamide and iodide ions on the corrosion inhibition of mild steel in H_2SO_4, *Materials Chemistry and Physics*, Vol. 106, 2007, pp. 387–393.

[10]. D.-Q. Zhang, L-X. Gao, G.-D. Zhou, Synergistic effect of 2-mercapto benzimidazole and KI on copper corrosion inhibition in aerated sulfuric acid solution, *J. Appl. Electrochem.*, Vol. 33, 2003, pp. 361–366.

[11]. Y. C. Wu, P. Zhang, H. W. Pickering, D. L. Alara, Effect of KI on improving copper corrosion inhibition efficiency of benzotriazole in sulfuric acid electrolytes, *J. Electrochem. Soc.*, Vol. 140, 1993, pp. 2791–2800.

[12]. D. Q. Zhang, X.-M. He, Q. R. Cai, L. X Gao, G. S. Kim, Corrosion inhibition and adsorption behavior of methionine on copper in HCl and synergistic effect of zinc ions, *Electrochem.*, Vol. 39, 2009, pp. 1193–1198.

[13]. E. E. Oguzie, Y. Li, F. H. Wang, Effect of surface nanocrystallization on corrosion and corrosion inhibition of low carbon steel: synergistic effect of methionine and iodide ion, *Electrochimica Acta*, Vol. 52, 2007, pp. 6988–6996.

[14]. K. F. Khaled, Corrosion control of copper in nitric acid solutions using some amino acids. A combined experimental and theoretical study, *Corrosion Science*, Vol. 52, 2010, pp. 3225–3234.

[15]. K. F. Khaled, M. A. Amin, Dry and wet lab studies for some benzotriazole derivatives as possible corrosion inhibitors for copper in 1.0 M HNO_3, *Corrosion Science*, Vol. 51, 2009, pp. 2098–2106.

[16]. K. F. Khaled, S. A. Fadl-Allah, B. Hammouti, Some benzotriazole derivatives as corrosion inhibitors for copper in acidic medium: experimental and quantum chemical molecular dynamics approach, *Materials Chemistry and Physic*, Vol. 117, 2009, pp. 148–155.

[17]. G. Quartarone, G. Moretti, T. Bellomi, G. Capobianco, A. Zingales, Using indole to inhibit copper corrosion in aerated 0.5 M sulphuric acid, *Corrosion Science*, Vol. 54, 1998, pp. 606.

[18]. X. Wu, H. Ma, S. Chen, Z. Xu, A. Sui, Studies on Electrochemical Behavior of Copper in Aerated NaBr Solutions with Schiff Base, N, N0-o-phenylen-bis(3-methoxysalicylidenimine*), Journal of the Electrochemical Society*, Vol. 148, 1999, pp. B208–B216.

[19]. K. F. Khaled, Monte Carlo simulations of corrosion inhibition of mild steel in 0.5 M sulphuric acid by some green corrosion inhibitors, *J Solid State Electrochem*, Vol. 13, 2009, pp. 1743–1756.

[20]. S. F. Mertens, C. Xhoffer, B. C. De Cooman, and E. Temmerman, .Short-term deterioration of polymer-coated 55% Al-Zn—part 1: behavior of thin polymer films, *Corrosion Science*, Vol. 53, Issue 5, 1997, pp. 381–387.

[21]. L. M. Rodriguez-Valdez, A. Martinez-Villafane, D. Glossman-Matnik, CHIH-DFT theoretical study of isomeric thiatriazoles and their potential activity as corrosion inhibitors, *J. Mol. Struct. THEOCHEM*, Vol. 713, 2005, pp. 65.

[22]. E. A. Noor, A. H. Al-Moubaraki, Thermodynamic study of metal corrosion and inhibitor adsorption processes in mild steel/1-methyl-4[4′(-X)-styrylpyridiniumiodides/hydrochloric acid systems, *Mater. Chem. Phys.*, Vol. 110, 2008, pp. 145–154.

[23]. A. K. Satpati and A. V. R. Reddy, Electrochemical study on corrosion inhibition of copper in hydrochloric acid medium and the rotating ring-disc voltammetry for studying the dissolution, *International Journal of Electrochemistry*, 2011, pp. 1- 8.

[24]. B. V. Appa Rao, Md. YakubIqbal, B. Sreedhar, Electrochemical and surface analytical studies of the self-assembled monolayer of 5-methoxy-2-(octadecylthio)benzimidazole in corrosion protection of copper, *Electrochimica Acta*, Vol. 55, 2010, pp. 620–631.

[25]. M. Cubillos, M. Sancy, J. Pavez, E. Vargas, R. Urzua, J. Henríquez-Romanc. Tribollet, J. H. Zagal, M. A. Páez, Influence of 8-aminoquinoline on the corrosion behaviour of copper in 0.1 M NaCl, .*Electrochimica Acta*, Vol. 55, 2010, pp. 2782–2792.

[26]. L. Larabi, O. BenalI, S. M. Meklleche, Hareky, 2-mercapto-1-methylimidazole as corrosion inhibitors for copper in hydrochloric acid, *Science Direct,* Vol. 86, 2006, pp. 1-8.

[27]. K. Barouni , L. Bazzi, R. Salghi, M. Mihit, B. Hammouti, A. Albourine S. El Issami, Some amino acids as corrosion inhibitors for copper in nitric acid solution. *Materials Letters*, Vol. 62, 2008, pp. 3325–3327.

[28]. H. Ma, S. Chen, L. Niu, S. Zhao, S. Li, D. Li, Inhibition of copper corrosion by several Schiff bases in aerated halide solutions, *Journal of Applied Electrochemistry*, Vol. 32, 2002, pp. 65–72.

[29]. X. Wu, H. Ma, S. Chen, Z. Xu, A. Sui, Studies on Electrochemical Behavior of Copper in Aerated NaBr Solutions with Schiff Base, N, N0-o-phenylen-bis(3-methoxysalicylidenimine), *Journal of the Electrochemical Society*, Vol. 148, 1999, pp. 208–216.

[30]. K. Aramaki, N. Hackerman, Inhibition Mechanism of Medium-Sized Polymethyl-Eneimine, *J. Electrochem. Soc.*, Vol. 116, 1969, pp. 568-574.

_____